
^{18}F -FET PET Compared with ^{18}F -FDG PET and CT in Patients with Head and Neck Cancer

Dirk Pauleit, MD^{1,2}; Andre Zimmermann, MD³; Gabriele Stoffels, MD¹; Dagmar Bauer, PhD¹; Jörn Risse, MD²; Michael O. Flüss, MD⁴; Kurt Hamacher, PhD⁵; Heinz H. Coenen, PhD⁵; and Karl-Josef Langen, MD¹

¹Institute of Medicine and Brain Imaging Center West, Research Center Jülich, Jülich, Germany; ²GP Nuclear Medicine and Radiology, Bad Honnef, Germany; ³Department of Cranio- and Maxillofacial Surgery, Heinrich-Heine University, Düsseldorf, Germany; ⁴Institute of Radiology, Heinrich-Heine University, Düsseldorf, Germany; and ⁵Institute of Nuclear Chemistry, Research Center Jülich, Jülich, Germany

Recent studies suggest a somewhat selective uptake of O-(2-[^{18}F]fluoroethyl)-L-tyrosine (FET) in cerebral gliomas and in squamous cell carcinoma (SCC) and a good distinction between tumor and inflammation. The aim of this study was to investigate the diagnostic potential of ^{18}F -FET PET in patients with SCC of the head and neck region by comparing that tracer with ^{18}F -FDG PET and CT. **Methods:** Twenty-one patients with suspected head and neck tumors underwent ^{18}F -FET PET, ^{18}F -FDG PET, and CT within 1 wk before operation. After coregistration, the images were evaluated by 3 independent observers and an ROC analysis was performed, with the histopathologic result used as a reference. Furthermore, the maximum standardized uptake values (SUVs) in the lesions were determined. **Results:** In 18 of 21 patients, histologic examination revealed SCC, and in 2 of these patients, a second SCC tumor was found at a different anatomic site. In 3 of 21 patients, inflammatory tissue and no tumor were identified. Eighteen of 20 SCC tumors were positive for both ^{18}F -FDG uptake and ^{18}F -FET uptake, one 0.3-cm SCC tumor was detected neither with ^{18}F -FDG PET nor with ^{18}F -FET PET, and one 0.7-cm SCC tumor in a 4.3-cm ulcer was overestimated as a 4-cm tumor on ^{18}F -FDG PET and missed on ^{18}F -FET PET. Inflammatory tissue was positive for ^{18}F -FDG uptake (SUV, 3.7–4.7) but negative for ^{18}F -FET uptake (SUV, 1.3–1.6). The SUVs of ^{18}F -FDG in SCC were significantly higher (13.0 ± 9.3) than those of ^{18}F -FET (4.4 ± 2.2). The ROC analysis showed significantly superior detection of SCC with ^{18}F -FET PET or ^{18}F -FDG PET than with CT. No significant difference ($P = 0.71$) was found between ^{18}F -FDG PET and ^{18}F -FET PET. The sensitivity of ^{18}F -FDG PET was 93%, specificity was 79%, and accuracy was 83%. ^{18}F -FET PET yielded a lower sensitivity of 75% but a substantially higher specificity of 95% (accuracy, 90%). **Conclusion:** ^{18}F -FET may not replace ^{18}F -FDG in the PET diagnostics of head and neck cancer but may be a helpful additional tool in selected patients, because ^{18}F -FET PET might better differentiate tumor tissue from inflammatory tissue. The sensitivity of ^{18}F -FET PET in SCC, however, was inferior to that of ^{18}F -FDG PET because of lower SUVs.

Key Words: ^{18}F -FET; ^{18}F -FDG; head and neck cancer; squamous cell carcinoma; amino acids; PET

J Nucl Med 2006; 47:256–261

Head and neck carcinoma constitutes approximately 5% of all malignancies, and its frequency is increasing (1). Squamous cell carcinoma (SCC) is the major histologic type of neoplasm arising from the head and neck area (2). The effectiveness of surgical treatment depends on the complete excision of all tumor tissue, and accurate preoperative staging is therefore mandatory. Detection of extension into adjacent tissues and structures is important and is usually done by anatomic imaging techniques, for example, CT and MRI. However, discrimination between tumor and reactive tissue changes may be difficult based solely on morphologic criteria (3). The sensitivity of anatomic imaging ranges from 67% to 88%, and the specificity, from 50% to 75% (4).

PET using 2- ^{18}F -FDG has been applied in many studies as an alternative imaging method and has been observed to improve preoperative diagnosis, with a sensitivity of 80%–100% for the detection of primary tumors, tumor recurrences, and occult metastases (4–10). ^{18}F -FDG, however, is not specific for cancer cells and exhibits high uptake in macrophages, fibroblasts, and granulation tissue (11,12). Thus, some studies report a specificity of only 60% for ^{18}F -FDG PET, especially after radiotherapy (6,13–16).

Radiolabeled amino acids such as L-[methyl- ^{11}C]methionine (MET) and L-1-[^{11}C]tyrosine (TYR), which are less avidly metabolized by inflammatory cells (17,18), have been explored as an alternative tracer for PET studies in patients with head and neck cancer. High sensitivity for the detection of these tumors has been reported for both tracers, and a specificity of 100% has been claimed especially for ^{11}C -TYR (18,19). Because of the short physical half-life of the ^{11}C label (20 min), however, ^{11}C -MET and ^{11}C -TYR remain restricted to a few PET centers with a cyclotron on site and cannot become established in routine clinical practice.

Received Jul. 20, 2005; revision accepted Oct. 31, 2005.

For correspondence or reprints contact: Dirk Pauleit, MD, Institute of Medicine, Research Center Jülich, P.O. Box 1913; 52425 Jülich, Germany.
E-mail: pauleit@web.de

Amino acids labeled with ^{18}F (half-life, 110 min), such as *O*-(2-[^{18}F]fluoroethyl)-L-tyrosine (FET), are presently under investigation in order to overcome the logistic disadvantages of ^{11}C -labeled amino acids. ^{18}F -FET can be synthesized with high radiochemical yields and can be produced on a large scale for clinical purposes (20,21). This artificial amino acid is not incorporated into proteins but exhibits high uptake in tumor cells because of increased transport via the amino acid transport systems L and B^{0,+} (20,22). ^{18}F -FET has successfully been applied to brain tumors, and convincing results have been reported for imaging the extent of gliomas, detecting recurrences, and differentiating gliomas from benign lesions (23–27). In addition, animal experiments have shown that ^{18}F -FET, in contrast to ^{18}F -FDG and ^{11}C -MET, exhibits no uptake in inflammatory cells or in inflammatory lymph nodes, thus promising a higher specificity for the detection of tumor cells (28,29).

Recently, we studied the diagnostic performance of ^{18}F -FET PET in different types of peripheral tumors (30). Surprisingly, no uptake of ^{18}F -FET could be detected in the majority of peripheral tumors, especially in lymphomas and most adenocarcinomas. This finding is in contrast to the results with other tyrosine derivatives (30). Most peripheral tumors that showed a high accumulation of ^{18}F -FET turned out to be SCC tumors.

The purpose of this study was to further investigate the diagnostic potential of ^{18}F -FET PET in patients with SCC of the head and neck region by comparing that tracer with ^{18}F -FDG PET and conventional morphologic imaging using CT.

MATERIALS AND METHODS

Patients

Twenty-one consecutive patients (3 women and 18 men; age range, 41–80 y; mean, 61 y) with suspected squamous head and neck cancer participated in this study. Data for the individual patients are given in Table 1. The mean size of the carcinoma tumors ($n = 20$) was 3.3 ± 2.1 cm (range, 0.3–8.3 cm), and that of the lymph node metastases ($n = 5$) was 1.1 ± 0.6 cm (range, 0.2–1.8 cm). The study was approved by the university ethics committee and by federal authorities. All subjects gave written informed consent to participate in the study.

Histopathologic Examination

All resected tissues were exactly localized and documented at each level to allow correlation between histopathologic findings and preoperative imaging results. Classification of the primary tumor and regional lymph node metastases was based on the TNM system (31).

Radiopharmaceuticals

The amino acid derivative ^{18}F -FET was produced via anion-activated nucleophilic ^{18}F -fluorination of *N*-trityl-*O*-(2-tosyl-oxyethyl)-L-tyrosine tert-butyl ester and subsequent deprotection. The uncorrected yield was about 35% at a specific radioactivity of greater than 200 GBq/ μmol and radiochemical purity of greater than 98% by optimizing our previous method (32). The tracer was administered as an isotonic neutral solution.

^{18}F -FDG was synthesized as previously described (32). The average specific radioactivity was greater than 200 GBq/ μmol .

PET

All patients fasted for at least 12 h before the PET studies. PET scanning started 1 h after intravenous injection of 370 MBq of ^{18}F -FET. Within 1 wk, all patients underwent comparative

TABLE 1
Data for Individual Patients and SUVs for ^{18}F -FDG and ^{18}F -FET in Primary Lesions

Patient no.	Sex	Age (y)	Histologic type	Stage	Location	Size (cm)	^{18}F -FDG SUV	^{18}F -FET SUV
1	M	52	SCC	pT1 N0	Oral cavity	0.7 in 4.3 ulcer	5.2	1.5
2	M	64	SCC	pT2 N0	Oral cavity	2.5	21.5	4.0
3	M	45	SCC	pT2 N2c	Oral cavity	4.0	14.8	3.5
4	M	59	SCC	pT2 N2b	Oral cavity	3.5	12.0	4.0
5	M	51	SCC	pT2 N1	Oropharynx	6.1	8.4	2.8
6	M	60	SCC	pT4b N1	Oral cavity	1.8	7.5	2.8
7	M	47	SCC	pT3 N0	Parotid gland	5.4	17.8	7.2
8	M	41	SCC	pT2 N0	Maxillary sinus	2.5	7.7	4.3
9	M	79	SCC	pT4a N0	Oral cavity	2.5	44.3	8.7
10	F	48	SCC	pT1 N0	Oral cavity	0.8	4.4	2.7
11	M	68	SCC	pT2 N0	Oral cavity	3.2	14.3	4.3
12	M	72	SCC	pT2 N1	Oral cavity	3.5	8.0	3.6
13	M	80	Inflammation		Oral cavity	3.0	3.7	1.6
14	M	63	SCC	pT3 N0	Oropharynx	8.0	21.5	5.0
			SCC	pT2 N0	Hypopharynx	2.7	8.0	3.8
15	F	74	SCC	pT1 N0	Oral cavity	0.3	1.8	0.9
16	M	49	Inflammation		Oropharynx	1.0	4.0	1.4
17	M	68	SCC	pT4 N0	Oral cavity	4.5	7.4	3.3
18	M	73	SCC	pT2 N0	Oral cavity	3.5	11.7	9.2
19	M	74	SCC	pT1 N0	Oral cavity	1.8	11.6	4.8
20	M	50	Inflammation		Oral cavity	1.2	4.7	1.3
21	F	73	SCC	pT3 N0	Oral cavity	8.3	20.7	7.4

investigations using the same scanning protocol. Blood glucose levels were checked before ^{18}F -FDG injection to ensure that they were less than 130 mg/dL.

The studies were performed on an ECAT EXACT HR+ scanner (CTI; optimum full width at half maximum, 4.5 mm; 15-cm transaxial field of view). For attenuation correction, transmission scans with three $^{68}\text{Ge}/^{68}\text{Ga}$ rotating line sources were used. After correction for random and scattered coincidences, dead time, and decay, image data were obtained by iterative reconstruction. Data were reconstructed with the manufacturer-supplied attenuation-corrected ordered-subsets expectation maximization algorithm including attenuation correction as described previously (30).

CT

Contrast-enhanced CT was performed as a routine preoperative procedure in all patients within 1 wk. Using a helical CT scanner (Somatom Plus 4; Siemens; slice thickness, 3 mm; pitch, 1.5; current, 100 mAs; potential, 120 kV), scans were acquired from the base of the skull to the apex of the chest.

Data Analysis

The data were evaluated after coregistration of the ^{18}F -FET PET, ^{18}F -FDG PET, and CT scans using dedicated software (MPI tool, version 3.28; ATV) (33).

First, similarly sized regions of interest were placed over the lesions on coregistered ^{18}F -FDG and ^{18}F -FET PET scans. Standardized uptake values (SUVs) of ^{18}F -FET and ^{18}F -FDG were calculated by dividing the maximum radioactivity (kBq/mL) of the regions of interest by the radioactivity injected per gram of body weight in the corresponding PET scans. For comparison of ^{18}F -FET SUVs with ^{18}F -FDG SUVs, the nonparametric *U* test of Mann and Whitney was used.

Second, we performed an alternative free-response receiver-operating-characteristic (ROC) analysis, which somewhat reflected the decision process in routine clinical practice and allowed for recording of the degree of confidence in making a decision. ^{18}F -FET PET, ^{18}F -FDG PET, and CT images were presented separately to 3 observers, each of whom was a nuclear medicine and radiology specialist and experienced in CT and PET reading. The images were randomly assigned to each observer, who had no knowledge of clinical information. In the first session, the observers reviewed the CT images, in the second session the ^{18}F -FDG PET images, and in a third session the ^{18}F -FET PET images.

For each patient, the observers evaluated 5 anatomic regions or levels (level 1, nasopharynx; level 2, oropharynx; level 3, hypopharynx/larynx; region 4, right cervical lymph nodes; region 5, left cervical lymph nodes), making 315 decisions on the presence of tumor on the presented images. Each observer recorded suspected lesions and gave each level a confidence rating based on a

6-point scale as follows: 6, definitely positive (when an observer was convinced that a lesion was a tumor); 5, probably positive (when an observer was not convinced that a lesion was a tumor but found it substantially likely to be a tumor); 4, possibly positive (when an observer was nearly undecided but tended to classify a lesion as being a tumor); 3, possibly negative (when an observer was nearly undecided but tended to classify a lesion as not being a tumor); 2, probably negative (when an observer was not convinced that a lesion was not a tumor but found it substantially likely to be nontumor tissue); and 1, definitely negative for tumor tissue (when an observer was convinced that there was no tumor). For the determination of sensitivity, specificity, and accuracy, a rating score of 4 or greater was considered positive for tumor tissue. Composite ROC curves were used to represent the performance of all observers as a group and were calculated by averaging the scores assigned by each of the observers. Alternative free-response ROC curves were generated for each imaging modality. The diagnostic accuracies were determined by calculating the area under the ROC curve (A_z) using dedicated ROC evaluation software (Rockit 0.9B; Charles E. Metz, University of Chicago). Differences between ROC curve integrals were tested for significance using the 2-tailed area test (a univariate *z* score test of the difference between the A_z values, with the null hypothesis that the datasets arose from binominal ROC curves with equal areas beneath them). Probability values of less than 0.05 were considered significant.

RESULTS

^{18}F -FET and ^{18}F -FDG Uptake

In 18 of 21 patients, histologic examination revealed SCC, and in 2 of these patients, a second SCC tumor was found at a different anatomic site. In 3 of 21 patients, inflammatory tissue and no tumor were identified by histology. Detailed data for each patient are given in Table 1. Eighteen of 20 SCC tumors were positive for ^{18}F -FDG and ^{18}F -FET uptake (Fig. 1). One 0.3-cm tumor was detected neither with ^{18}F -FDG PET nor with ^{18}F -FET PET. In a different patient, histologic examination showed a 0.7-cm tumor in a 4.3-cm inflammatory ulcer (Fig. 2). The ^{18}F -FDG PET scan overestimated the carcinoma as a 4-cm lesion with increased ^{18}F -FDG uptake (SUV, 5.2), and the scan obtained with ^{18}F -FET (SUV, 1.5) missed this small carcinoma. All carcinomas with increased ^{18}F -FET uptake exhibited concordant ^{18}F -FDG accumulation, and no additional lesion could be identified with ^{18}F -FET PET. The SUVs for SCC were higher in all cases with ^{18}F -FDG than with ^{18}F -FET; the mean SUV for ^{18}F -FDG was 13.0 ± 9.3 (range, 1.8–44.3) and that for



FIGURE 1. ^{18}F -FDG PET (A), CT (B), and ^{18}F -FET PET (C) images of 72-y-old man with SCC of oral cavity (arrows). Tumor exhibits increased uptake of ^{18}F -FDG (SUV, 8.0) and ^{18}F -FET (SUV, 3.6).

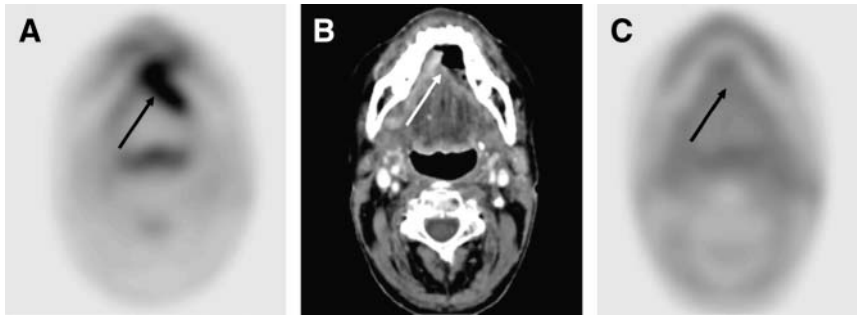


FIGURE 2. ^{18}F -FDG PET (A), CT (B), and ^{18}F -FET PET (C) images of 52-y-old man with 0.7-cm SCC in 4.3-cm ulcer with inflammatory tissue (arrows). ^{18}F -FDG PET scan shows approximately 4-cm lesion with increased ^{18}F -FDG uptake (SUV, 5.2) that allows no discrimination between carcinoma and inflammation. CT scan demonstrates air-filled ulcer, and ^{18}F -FET PET scan reveals no abnormal ^{18}F -FET uptake (SUV, 1.5), missing the small carcinoma.

^{18}F -FET was 4.4 ± 2.2 (range, 0.9–9.2) ($P < 0.001$). In the lymph node metastases ($n = 5$), with an average size of 1.1 ± 0.6 cm, no increased ^{18}F -FET uptake could be identified (mean SUV, 1.4 ± 0.3 ; range, 1.0–1.9). The corresponding SUV for ^{18}F -FDG uptake ranged from 1.6 to 3.3 (mean, 2.3 ± 0.7); 2 of 5 lymph node metastases had an SUV above 2.5 and 3 of 5 had an SUV below 2.5. Important to note is that inflammatory tissue showed an increased uptake of ^{18}F -FDG, with the SUV increasing from 3.7 to 4.7, which is within the range of ^{18}F -FDG uptake in SCC. In contrast, no increased accumulation of ^{18}F -FET was found in inflammatory tissue (SUV range, 1.3–1.6) (Fig. 3).

ROC Analysis

The alternative free-response ROC curves formed on the basis of pooled data from the 3 observers are shown in Figure 4. The A_z values for CT, ^{18}F -FET PET, and ^{18}F -FDG PET were 0.82, 0.93, and 0.95, respectively.

Detection of SCC was significantly ($P < 0.05$) better using ^{18}F -FET PET or ^{18}F -FDG PET than using routine anatomic imaging with CT. For ^{18}F -FDG PET and ^{18}F -FET PET, no significant difference ($P = 0.71$) in A_z values could be identified.

When a rating of 1–3 on the 6-point rating scale was considered negative for tumor tissue and a rating of 4 or higher was considered positive for tumor tissue, the sensitivity of ^{18}F -FDG PET was 93% but specificity was only 79% (accuracy, 83%). ^{18}F -FET PET yielded a lower sensitivity of 75% but a substantially higher specificity of 95% (accuracy, 90%). CT achieved a sensitivity of 64%, a specificity of 86%, and the lowest accuracy, 80%.

DISCUSSION

The aim of this prospective study was to explore the diagnostic potential of ^{18}F -FET PET in patients with primary SCC of the head and neck region by comparing that tracer with ^{18}F -FDG PET and CT. Detection of SCC was not better with ^{18}F -FET PET than with ^{18}F -FDG PET, and no significant difference in accuracy was identified in an ROC analysis. An important finding was that the specificity of ^{18}F -FET PET for the detection of SCC was superior to that of ^{18}F -FDG PET and CT. We suggest that this difference is caused by the increased uptake of ^{18}F -FDG in physiologic tissue of the head and neck region and in inflammatory tissue. In contrast to ^{18}F -FDG, ^{18}F -FET was not taken up by inflammatory tissue—an observation that is in line with the results of animal experiments (28,29) and with our observations in a previous study (30) (Fig. 3). A drawback of ^{18}F -FET PET, however, was the low sensitivity, only 75%, in this series of patients. The differences in sensitivity and specificity may be attributed partly to the relatively low ^{18}F -FET uptake in the tumors. This low uptake leads to a poorer detection rate, especially in small tumors, which are missed because of partial-volume effects. All larger SCC tumors confirmed our previous findings (30) by demonstrating an increased uptake of ^{18}F -FET. However, the higher sensitivity of ^{18}F -FDG in SCC may also be influenced by the high tracer uptake in the concomitant inflammation, as is nicely illustrated in the case of patient 1 (Fig. 2). In that patient, a 0.7-cm tumor was found in a 4.3-cm ulcer and, because of high uptake in the inflammatory process, was rated positive for ^{18}F -FDG uptake whereas ^{18}F -FET PET was negative.



FIGURE 3. ^{18}F -FDG PET (A), CT (B), and ^{18}F -FET PET (C) images of 50-y-old man with chronic inflammatory tissue (arrows). ^{18}F -FDG PET scan shows lesion with increased ^{18}F -FDG uptake (SUV, 4.7) suggesting malignancy. ^{18}F -FET PET was true negative, with no increased ^{18}F -FET uptake (SUV, 1.3).

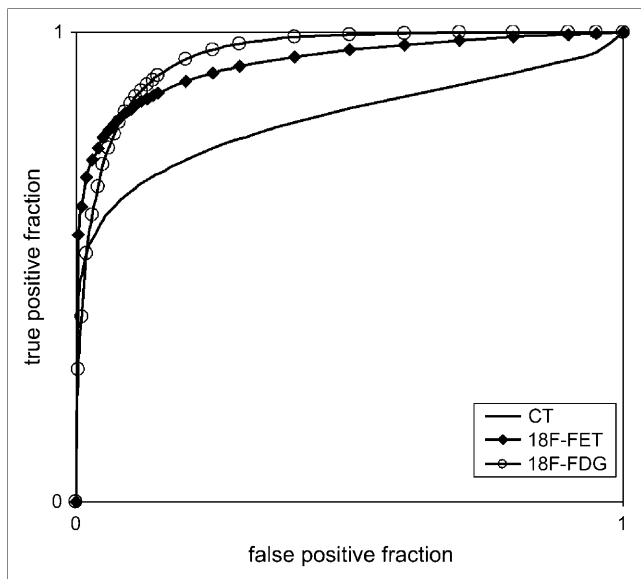


FIGURE 4. Composite ROC curves of the 3 observers. A_z values for CT, ^{18}F -FET PET, and ^{18}F -FDG PET were 0.82, 0.93, and 0.95, respectively. Accuracy of observers did not significantly differ ($P = 0.71$) between ^{18}F -FDG and ^{18}F -FET PET but, in the distinction of carcinomas, was significantly ($P < 0.05$) greater with either technique than with CT.

The reason for the somewhat selective accumulation of ^{18}F -FET in certain tumor types and the low uptake in inflammatory tissue has not yet been fully explained. In a previous study, we speculated that a selective transport of ^{18}F -FET via subtype 2 of the L-type amino acid transporter (LAT) might account for this phenomenon (30). A study expressing different subtypes of LAT in *Xenopus* oocytes has shown that the natural amino acid L-tyrosine is transported by both subtype 1 and subtype 2 (34). Another study demonstrated that ^{18}F -FET influx via subtype 1 is poor, indicating that LAT-like transport may occur mainly via subtype (35). This transporter subtype, however, appears not to be expressed in inflammatory tissue (36), possibly explaining the low uptake of ^{18}F -FET in such tissue.

The observation of a higher selectivity of ^{18}F -FET for certain amino acid transporters compared with its natural parent is a rather interesting finding. A similar phenomenon has been observed for the radioiodinated tyrosine derivative L-3- ^{123}I -iodo- α -methyl-tyrosine, which is selectively transported by subtype 1 of LAT (34). The further development of such amino acids may help in the exploration of dysregulations of specific amino acid transporters and their involvement in the pathogenesis of various diseases.

Although the SUVs for ^{18}F -FET were significantly lower than those for ^{18}F -FDG, the uptake values were similar to those reported for ^{11}C -TYR PET, for which a sensitivity and specificity of 100% for the detection of SCC of the head and neck region has recently been claimed by a group of investigators (18,37). An earlier publication on SCC by the same group, however, reported that ^{11}C -TYR accumulated in several lymph nodes that were normal on histo-

pathologic examination (38). Thus, some doubt of the high specificity of ^{11}C -TYR accumulation in SCC appears warranted, and additional uptake in concomitant inflammation has to be considered. Furthermore, high uptake in the salivary glands constitutes a major problem for ^{11}C -TYR PET and ^{11}C -MET PET and makes the detection of tumors near these glands difficult (18,39). Recent studies have reported that, because of high unspecific uptake and overestimation of tumor volumes, ^{11}C -MET PET was not helpful in determining tumor volumes for the planning of radiation therapy for head and neck tumors (40). The high uptake of ^{11}C -TYR and ^{11}C -MET in the salivary glands might be explained by the fact that these tracers are incorporated into proteins that are synthesized in large amounts in these glands. In contrast, ^{18}F -FET is not incorporated into proteins, and no uptake was noted in the salivary glands.

Because uptake and sensitivity are lower for ^{18}F -FET than for ^{18}F -FDG, ^{18}F -FET does not represent an ideal tracer for the evaluation of primary SCC of the head and neck region. Also, the detection rate of ^{18}F -FET PET for lymph nodes in the present study appeared to be lower than that of ^{18}F -FDG PET, although the number of positive lymph nodes in this series of patients was too small to allow for definitive conclusions. Nevertheless, the higher specificity makes ^{18}F -FET PET an interesting additional tool in the follow-up of patients with SCC. A possible application of ^{18}F -FET PET may be the monitoring of radio- or chemotherapy of SCC, because the reaction of the tumor tissue may be specifically detected without the interfering uptake by inflammatory or reactive tissue. Especially in pretreated patients in whom CT or MRI cannot differentiate a recurrent tumor from reactive changes, a reliable noninvasive imaging method may be helpful. Although a biopsy should be performed in cases of clinical suspicion, repeatedly negative biopsies may not exclude the presence of viable tumor, and the trauma caused by biopsies on irradiated tissue may initiate infection, further edema, and failure to heal (5). Further clinical studies are needed to elucidate the possible role of ^{18}F -FET PET in this context.

CONCLUSION

^{18}F -FET may not replace ^{18}F -FDG in the PET diagnostics of head and neck cancer but may be a helpful additional tool in selected patients by allowing better differentiation of tumor tissue from inflammatory tissue. The sensitivity of ^{18}F -FET PET in SCC, however, was inferior to that of ^{18}F -FDG PET because of lower SUVs.

ACKNOWLEDGMENTS

The authors thank Bettina Palm, Erika Wabbals, and Silke Grafmüller for technical assistance in the radiosynthesis of ^{18}F -FET, and Elisabeth Theelen and Suzanne Schaden for assistance with patient studies and data analysis.

REFERENCES

- Parker SL, Tong T, Bolden S, et al. Cancer statistics: 1996. *CA Cancer J Clin*. 1996;46:5–27.
- Vokes EE, Weichselbaum RR, Lippman SM, et al. Head and neck cancer. *N Engl J Med*. 1993;328:184–194.
- Di Martino E, Rieger M, Hassan HA, et al. Multiple primary carcinomas in patients with head and neck malignancies. *Laryngorhinootologie*. 2000;79:711–718.
- Hain SF. Positron emission tomography in cancer of the head and neck. *Br J Oral Maxillofac Surg*. 2005;43:1–6.
- Brouwer J, de Bree R, Comans EF, et al. Positron emission tomography using [¹⁸F]fluorodeoxyglucose (FDG-PET) in the clinically negative neck: is it likely to be superior? *Eur Arch Otorhinolaryngol*. 2004;261:479–483.
- Kunkei M, Forster GJ, Reichert TE, et al. Detection of recurrent oral squamous cell carcinoma by [¹⁸F]-2-fluorodeoxyglucose-positron emission tomography: implications for prognosis and patient management. *Cancer*. 2003;98:2257–2265.
- McGuirt WF, Greven K, Williams D III, et al. PET scanning in head and neck oncology: a review. *Head Neck*. 1998;20:208–215.
- Brun E, Kjellen E, Tennvall J, et al. FDG PET studies during treatment: prediction of therapy outcome in head and neck squamous cell carcinoma. *Head Neck*. 2002;24:127–135.
- Teknos TN, Rosenthal EL, Lee D, et al. Positron emission tomography in the evaluation of stage III and IV head and neck cancer. *Head Neck*. 2001;23:1056–1060.
- Dammann F, Horger M, Mueller-Berg M, et al. Rational diagnosis of squamous cell carcinoma of the head and neck region: comparative evaluation of CT, MRI, and ¹⁸F-FDG PET. *AJR*. 2005;184:1326–1331.
- Kubota R, Yamada S, Kubota K, et al. Intratumoral distribution of fluorine-18-fluorodeoxyglucose in vivo: high accumulation in macrophages and granulation tissues studied by microautoradiography. *J Nucl Med*. 1992;33:1972–1980.
- Reinhardt MJ, Kubota K, Yamada S, et al. Assessment of cancer recurrence in residual tumors after fractionated radiotherapy: a comparison of fluorodeoxyglucose, L-methionine and thymidine. *J Nucl Med*. 1997;38:280–287.
- Kresnik E, Mikosch P, Gallowitz HJ, et al. Evaluation of head and neck cancer with ¹⁸F-FDG PET: a comparison with conventional methods. *Eur J Nucl Med*. 2001;28:816–821.
- Sigg MB, Steinert H, Gratz K, et al. Staging of head and neck tumors: [¹⁸F]fluorodeoxyglucose positron emission tomography compared with physical examination and conventional imaging modalities. *J Oral Maxillofac Surg*. 2003;61:1022–1029.
- Greven KM, Keyes JW Jr, Williams DW III, et al. Occult primary tumors of the head and neck: lack of benefit from positron emission tomography imaging with 2-[¹⁸F]fluoro-2-deoxy-D-glucose. *Cancer*. 1999;86:114–118.
- Klabbers BM, Lammertsma AA, Slotman BJ. The value of positron emission tomography for monitoring response to radiotherapy in head and neck cancer. *Mol Imaging Biol*. 2003;5:257–270.
- Kubota R, Kubota K, Yamada S, et al. Methionine uptake by tumor tissue: a microautoradiographic comparison with FDG. *J Nucl Med*. 1995;36:484–492.
- de Boer JR, van der Laan BF, Pruim J, et al. Carbon-11 tyrosine PET for visualization and protein synthesis rate assessment of laryngeal and hypopharyngeal carcinomas. *Eur J Nucl Med Mol Imaging*. 2002;29:1182–1187.
- Lindholm P, Leskinen S, Lapela M. Carbon-11-methionine uptake in squamous cell head and neck cancer. *J Nucl Med*. 1998;39:1393–1397.
- Wester HJ, Herz M, Weber W, et al. Synthesis and radiopharmacology of O-(2-[¹⁸F]fluoroethyl)-L-tyrosine for tumor imaging. *J Nucl Med*. 1999;40:205–212.
- Hamacher K, Coenen HH. Efficient routine production of the ¹⁸F-labelled amino acid O-(2-[¹⁸F]fluoroethyl)-L-tyrosine. *Appl Radiat Isot*. 2002;57:853–856.
- Langen KJ, Jarosch M, Mühlensiepen H, et al. Comparison of fluorotyrosines and methionine uptake in F98 rat gliomas. *Nucl Med Biol*. 2003;30:501–508.
- Weber WA, Wester HJ, Grou AL, et al. O-(2-[¹⁸F]fluoroethyl)-L-tyrosine and L-[methyl-¹¹C]methionine uptake in brain tumours: initial results of a comparative study. *Eur J Nucl Med*. 2000;27:542–549.
- Pöpperl G, Gotz C, Rächinger W, Gildehaus FJ, Tonn JC, Tatsch K. Value of O-(2-[¹⁸F]fluoroethyl)-L-tyrosine PET for the diagnosis of recurrent glioma. *Eur J Nucl Med Mol Imaging*. 2004;31:1464–1470.
- Pauleit D, Floeth F, Hamacher K, et al. O-(2-[¹⁸F]fluoroethyl)-L-tyrosine PET combined with magnetic resonance imaging improves the diagnostic assessment of cerebral gliomas. *Brain*. 2005;128:678–687.
- Floeth FW, Pauleit D, Witsack HJ, et al. Multimodal metabolic imaging of cerebral gliomas: positron emission tomography with [¹⁸F]fluoroethyl-L-tyrosine and magnetic resonance spectroscopy. *J Neurosurg*. 2005;102:318–327.
- Weckesser M, Langen KJ, Rickert CH, et al. O-(2-[¹⁸F]fluoroethyl)-L-tyrosine PET in the clinical evaluation of primary brain tumors. *Eur J Nucl Med Mol Imaging*. 2005;32:422–429.
- Kaim AH, Weber B, Kurrer MO, et al. (¹⁸F)-FDG and (¹⁸F)-FET uptake in experimental soft tissue infection. *Eur J Nucl Med Mol Imaging*. 2002;29:648–654.
- Rau FC, Weber WA, Wester HJ, et al. O-(2-[¹⁸F]fluoroethyl)-L-tyrosine (FET): a tracer for differentiation of tumour from inflammation in murine lymph nodes. *Eur J Nucl Med Mol Imaging*. 2002;29:1039–1046.
- Pauleit D, Stoffels G, Schaden W, et al. PET with O-(2-[¹⁸F]fluoroethyl)-L-tyrosine (FET) in peripheral tumours: first clinical results. *J Nucl Med*. 2005;46:411–416.
- Sobin LH, Wittekind C, eds. *UICC-TNM Classification of Malignant Tumours*. 6th ed. New York, NY: Wiley-Liss; 2002.
- Hamacher K, Coenen HH, Stöcklin G. Efficient stereospecific synthesis of no-carrier-added 2-[¹⁸F]fluoro-2-deoxy-D-glucose using aminopolyether supported nucleophilic substitution. *J Nucl Med*. 1986;27:235–238.
- Pietrzyk U, Herholz K, Heiss WD. Three-dimensional alignment of functional and morphological tomograms. *J Comput Assist Tomogr*. 1990;14:51–59.
- Shikano N, Kanai Y, Kawai K, et al. Isoform selectivity of 3-¹²⁵I-iodo-alpha-methyl-L-tyrosine membrane transport in human L-type amino acid transporters. *J Nucl Med*. 2003;44:244–246.
- Lahoutte T, Caveliers V, Camargo SMR, et al. SPECT and PET amino acid tracer influx via system L (h4F2hc-hLat1) and its transstimulation. *J Nucl Med*. 2004;45:1591–1596.
- Rau FC, Philippi H, Rubio-Aliaga I, et al. Identification of subtypes of amino acid transporters in human tumor and inflammatory cells by RT-PCR [abstract]. *J Nucl Med*. 2002;43(suppl):24P.
- De Boer JR, Pruim J, Burlage F, et al. Therapy evaluation of laryngeal carcinomas by tyrosine-PET. *Head Neck*. 2003;25:634–644.
- Braams JW, Pruim J, Nikkels PGJ, et al. Nodal spread of squamous cell carcinoma of the oral cavity detected with PET-tyrosine, MRI and CT. *J Nucl Med*. 1996;37:897–901.
- Buus S, Grau C, Munk OL, et al. ¹¹C-methionine PET, a novel method for measuring regional salivary gland function after radiotherapy of head and neck cancer. *Radiother Oncol*. 2004;73:289–296.
- Geets X, Daisne JF, Gregoire V, et al. Role of ¹¹C-methionine positron emission tomography for the delineation of the tumor volume in pharyngo-laryngeal squamous cell carcinoma: comparison with FDG-PET and CT. *Radiother Oncol*. 2004;71:267–273.